

Branching ratios, CP asymmetries and polarizations of $B \rightarrow \psi(2S)V$ decays

Zhou Rui^{1,*}, Ya Li^{2,†} and Zhen-Jun Xiao^{2‡}

¹ *College of Sciences, North China University of Science and Technology, Tangshan 063009, China and*

² *Department of Physics and Institute of Theoretical Physics,
Nanjing Normal University, Nanjing 210023, Jiangsu, China*

(Dated: October 15, 2018)

We analyzed the nonleptonic decays $B/B_s \rightarrow \psi(2S)V$ with $V = (\rho, \omega, K^*, \phi)$ by employing the perturbative QCD (PQCD) factorization approach. Here the branching ratios, the CP asymmetries and the complete set of polarization observables are investigated systematically. Besides the traditional contributions from the factorizable and nonfactorizable diagrams at the leading order, the next-to-leading order (NLO) vertex corrections could also provide considerable contributions. The PQCD predictions for the branching ratios of the $B_{(s)} \rightarrow \psi(2S)K^*, \psi(2S)\phi$ decays are consistent with the measured values within errors. As for $B \rightarrow \psi(2S)\rho, \psi(2S)\omega$ decays, the branching ratios can reach the order of 10^{-5} and could be measured in the LHCb and Belle-II experiments. The numerical results show that the direct CP asymmetries of the considered decays are very small. Thus the observation of any large direct CP asymmetry for these decays will be a signal for new physics. The mixing induced CP asymmetries in the neutral modes are very close to $\sin 2\beta_{(s)}$, which suggests that these channels can give a cross-check on the measurement of the Cabibbo-Kobayashi-Maskawa (CKM) angle β and β_s . We found that the longitudinal polarization fractions f_0 are suppressed to $\sim 50\%$ due to the large nonfactorizable contributions. The magnitudes and phases of the two transverse amplitudes \mathcal{A}_{\parallel} and \mathcal{A}_{\perp} are roughly equal, which is an indication for the approximate light quark helicity conservation in these decays. The overall polarization observables of $B \rightarrow \psi(2S)K^{*0}$ and $B_s \rightarrow \psi(2S)\phi$ channels are also in good agreement with the experimental measurements as reported by LHCb and BaBar. Other results can also be tested by the LHCb and Belle-II experiments.

PACS numbers: 13.25.Hw, 12.38.Bx, 14.40.Nd

I. INTRODUCTION

Studies of the decays of B mesons into a charmonium meson plus a light vector meson contribute a lot to our knowledge about the CP violation and mixing in the B meson system [1], and also provide a particularly important place to look for the physics beyond the standard model (SM). For example, the mode $B_s^0 \rightarrow J/\psi\phi$ is the so-called “golden mode” for measuring β_s , which is extracted from the angular analysis of the time-dependent differential decay rate [2–4]. The counterpart phase β in the B meson system can also be extracted in $B^0 \rightarrow J/\psi K^*$ decay [5]. The decay $B^0 \rightarrow J/\psi\phi$, which would proceed mainly via a Cabibbo-suppressed and color-suppressed transition ($bd \rightarrow \bar{c}\bar{d}\bar{d}$) with rescattering of $d\bar{d}$ into $s\bar{s}$, provide useful information for understanding rescattering mechanisms [6–8]. In addition, combining the decays $B^0 \rightarrow J/\psi\phi$ and $B^0 \rightarrow J/\psi\omega$ can be helpful to study the $\omega - \phi$ mixing [9]. These decays are dominated by tree diagrams and the contributions from penguin diagrams are expected to be small. With continuously increasing high-precision measurements, the penguin effects, which play an important role in the extraction of the above phases, can be measured by means of an analysis of the angular distribution of $B^0 \rightarrow J/\psi\rho^0$ [10] and $B_s^0 \rightarrow J/\psi\bar{K}^{*0}$ [11].

In the framework of SM, these decay modes are induced by transitions $b \rightarrow qc\bar{c}$ with $q = d, s$. In principle, any mode involving various excitations of the $c\bar{c}$ mesons such as $B \rightarrow \psi(2S)V$ decays could be an alternative to that for J/ψ analogues, and give additional and complementary information. Experimentally, the $\psi(2S)$ meson can be reconstructed in the decay channels $\psi(2S) \rightarrow \mu^+\mu^-$ and $\psi(2S) \rightarrow J/\psi\pi^+\pi^-$, with the J/ψ meson decaying into two muons [12]. Nowadays, several experimental Collaborations have measured the decays $B_s^0 \rightarrow \psi(2S)\phi$ [13], $B \rightarrow \psi(2S)K^*(892)$ [14–18], $B^0 \rightarrow \psi(2S)\pi^0$ [19], $B^+ \rightarrow \psi(2S)\pi^+$ [20], $B_s \rightarrow \psi(2S)\eta^{(\prime)}$ [21, 22]. Some relative ratios

*Electronic address: jindui1127@126.com

†Electronic address: liyakelly@163.com

‡Electronic address: xiaozhenjun@njnu.edu.cn

of the branching ratios for B meson decays into $\psi(2S)$ and J/ψ mesons are also measured by several experiments [23–26].

On the theory side, these $B \rightarrow \psi(2S)V$ modes do have some special properties. Since there are three possible values of the total angular momentum with different CP eigenvalues ($L = 1$ is odd, while $L = 0, 2$ are even), the angular analysis is needed to separate the contributions from the CP -even and CP -odd partial waves. Therefore the final state can be decomposed into three helicity amplitudes (one longitudinal and two transverse components). The information about the phases of the transverse decay amplitudes provides a test of the factorization hypothesis [27]. Furthermore, $B \rightarrow \psi(2S)V$ are the color-suppressed modes and therefore a significant impact of nonfactorizable contributions is expected. Both improvements in the accuracy of the experimental measurements and the observation of new modes, especially involving $\psi(2S)$ in the final states, can be helpful in understanding the role of any nonfactorizable corrections [28–30] and differentiating various theory approaches. Nowadays there exist several theoretical approaches as described in Refs. [31–46] which shed more light on the S-wave ground state charmonium decays of B mesons. The nonleptonic B decays with radially excited charmonium mesons in final state, however, have received less attention in the literature.

Based on the k_T factorization theorem, The perturbative QCD (PQCD) approach [47, 48] is suitable for describing different types of heavy hadron decays. After including the parton transverse momentum k_T , which is not negligible in the end-point region, both factorizable and nonfactorizable contributions are calculable without endpoint singularity. The Sudakov resummation has also been introduced to suppress the long-distance contributions effectively. Therefore, the PQCD approach is a self-consistent framework and has a good predictive power. In our previous works [49–51], the semi-leptonic, two-body and three-body non-leptonic decays of the $B_c(B)$ mesons to $\psi(2S)$ are studied in the PQCD framework. Here, furthermore, we will extend our previous analysis to the $B \rightarrow \psi(2S)V$ decays. In a recent work [52], The authors applied the PQCD approach to study $B \rightarrow J/\psi V$ decays and also obtained the theoretical predictions in good agreement with currently available data. Therefore we have good reasons to believe that it is appropriate to analyze $B \rightarrow \psi(2S)V$ in this framework.

This work is organized as follows. In Sec. II we present some basic formulas such as the effective Hamiltonian and kinetic conventions, then briefly review the pQCD approach. The technical formulas of the calculation and the nonperturbative meson wave functions are summarised in Appendix A and B, respectively. Section III devoted to numerical calculation and discussion. Our conclusions are left for Sec. IV.

II. ANALYTIC FORMULAS AND PERTURBATIVE CALCULATIONS

For nonleptonic charmonium B decays, both the tree operators and the penguin operators of the standard effective weak Hamiltonian contribute, which is given by [53]

$$\mathcal{H}_{eff} = \frac{G_F}{\sqrt{2}} \{ \xi_c [C_1(\mu)O_1^c(\mu) + C_2(\mu)O_2^c(\mu)] - \xi_t \sum_{i=3}^{10} C_i(\mu)O_i(\mu) \}, \quad (1)$$

with the CKM matrix element $\xi_{c(t)} = V_{c(t)b}^* V_{c(t)q}$. $O_i(\mu)$ and $C_i(\mu)$ are the effective four quark operators and their QCD corrected Wilson coefficients at the renormalization scale μ , respectively. Their explicit form can be found in Ref. [53].

At quark level, when the $\bar{b} \rightarrow \bar{q}c\bar{c}$ decay occurs through the four quark operators, a $c\bar{c}$ state $\psi(2S)$ is created while the other light anti-quark \bar{q} is flying away. Since the heavy b quark in B meson carry most of the energy of B meson, the spectator quark of the B meson is soft. A hard gluon is exchanged so that the spectator quark gets energy from the four quark operator and then form a fast moving vector meson with its partner anti-quark. This makes the perturbative calculations into a six-quark interaction, which involves the four quark operator and the spectator quark connected by a hard gluon. The relevant Feynman diagrams are shown in Fig. 1.

In the PQCD approach, the decay amplitudes are expressed as the convolution of the hard kernels H with the relevant meson wave functions Φ_i

$$\mathcal{A}(B \rightarrow \psi(2S)V) = \int d^4k_1 d^4k_2 d^4k_3 Tr[C(t)\Phi_B(k_1)\Phi_{\psi(2S)}(k_2)\Psi_V(k_3)H(k_1, k_2, k_3, t)], \quad (2)$$

where k_i are the momentum of the quark in each meson, and “Tr” denotes the trace over all Dirac structure and color indices. $C(t)$ is the short distance Wilson coefficients at the hard-scale t . The meson wave functions Φ , including all nonperturbative components in the k_T factorization, can be extracted from experimental data or other nonperturbative methods. The hard kernel $H(k_i, t)$ describes the four quark operator and the spectator quark connected by a hard gluon, which can be perturbatively calculated including all possible Feynman diagrams without endpoint singularity. In the following, we start to compute the decay amplitudes of $B \rightarrow \psi(2S)V$ decay.

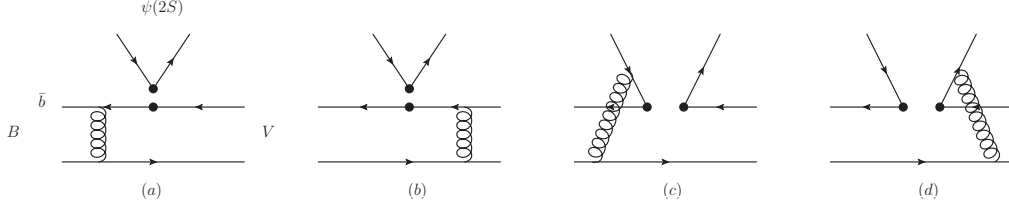


FIG. 1: The typical leading-order Feynman diagrams for the decay $B \rightarrow \psi(2S)V$. (a,b) The factorizable diagrams, and (c,d) the nonfactorizable diagrams.

We will work in the B meson rest frame and employ the light-cone coordinates for momentum variables. The B meson momentum P_1 , the $\psi(2S)$ meson momentum P_2 , the vector meson momentum P_3 and the quark momenta k_i in each meson are chosen as

$$\begin{aligned}
 P_1 &= \frac{M}{\sqrt{2}}(1, 1, \mathbf{0}_T), & P_2 &= \frac{M}{\sqrt{2}}(1 - r_v^2, r^2, \mathbf{0}_T), & P_3 &= \frac{M}{\sqrt{2}}(r_v^2, 1 - r^2, \mathbf{0}_T), \\
 k_1 &= \left(\frac{M}{\sqrt{2}}x_1, 0, \mathbf{k}_{1T}\right), & k_2 &= \left(\frac{M}{\sqrt{2}}x_2(1 - r_v^2), \frac{M}{\sqrt{2}}x_2r^2, \mathbf{k}_{2T}\right), & k_3 &= \left(\frac{M}{\sqrt{2}}x_3r_v^2, \frac{M}{\sqrt{2}}x_3(1 - r^2), \mathbf{k}_{3T}\right),
 \end{aligned} \quad (3)$$

with the mass ratio $r_{(v)} = m_{\psi(2S)}(m_V)/M$ and $m_{\psi(2S)}, m_V, M$ are the masses of the charmonium, vector meson and B meson, respectively. The k_{iT}, x_i represent the transverse momentum and longitudinal momentum fraction of the quark inside the meson. Since the final state consists of two spin-1 particles, to extract the helicity amplitudes, the following parametrization for the longitudinal and transverse polarization vectors is useful:

$$\begin{aligned}
 \epsilon_2^L &= \frac{1}{\sqrt{2(1 - r_v^2)}r}(1 - r_v^2, -r^2, \mathbf{0}_T), & \epsilon_2^T &= (0, 0, \mathbf{1}_T), \\
 \epsilon_3^L &= \frac{1}{\sqrt{2(1 - r^2)}r_v}(-r_v^2, 1 - r^2, \mathbf{0}_T), & \epsilon_3^T &= (0, 0, \mathbf{1}_T),
 \end{aligned} \quad (4)$$

which satisfy the normalization $(\epsilon_{2,3}^L)^2 = (\epsilon_{2,3}^T)^2 = -1$ and the orthogonality $\epsilon_2^L \cdot P_2 = \epsilon_3^L \cdot P_3 = 0$.

The decay amplitude can be decomposed into three parts of the polarizations amplitudes as follows:

$$\mathcal{A}(B \rightarrow \psi(2S)V) = \mathcal{A}_L + \mathcal{A}_N \epsilon_2^T \cdot \epsilon_3^T + i \mathcal{A}_T \epsilon_{\alpha\beta\rho\sigma} n^\alpha v^\beta \epsilon_2^{T\rho} \epsilon_3^{T\sigma}, \quad (5)$$

with the null vectors $n = (1, 0, \mathbf{0}_T)$ and $v = (0, 1, \mathbf{0}_T)$. The subscript L, N, T correspond to the longitudinal, normal and transverse polarization states, respectively. According to Eq. (1), the three different polarization amplitudes have the following expressions,

$$\begin{aligned}
 \mathcal{A}_{L,N,T}(B \rightarrow \psi(2S)V) &= \xi_c \left[(C_1 + \frac{1}{3}C_2) \mathcal{F}_{L,N,T}^{LL} + C_2 \mathcal{M}_{L,N,T}^{LL} \right] - \xi_t \left[(C_3 + \frac{1}{3}C_4 + C_9 + \frac{1}{3}C_{10}) \mathcal{F}_{L,N,T}^{LL} + \right. \\
 &\quad \left. (C_5 + \frac{1}{3}C_6 + C_7 + \frac{1}{3}C_8) \mathcal{F}_{L,N,T}^{LR} + (C_4 + C_{10}) \mathcal{M}_{L,N,T}^{LL} + (C_6 + C_8) \mathcal{M}_{L,N,T}^{SP} \right], \quad (6)
 \end{aligned}$$

where $\mathcal{F}(\mathcal{M})$ describes the contributions from the factorizable (nonfactorizable) diagrams. The superscript LL, LR , and SP refers to the contributions from $(V - A) \otimes (V - A)$, $(V - A) \otimes (V + A)$ and $(S - P) \otimes (S + P)$ operators, respectively. These explicit factorization formulas are all listed in Appendix A. In this work, we also consider the vertex corrections to the factorizable amplitudes \mathcal{F} at the current known next-to-leading order (NLO) level. Their effects can be combined in the Wilson coefficients as usual [54]. In the NDR scheme, the vertex corrections are included by the modifications to the combinations a_i ¹ of the Wilson coefficients C_i associated with the factorizable

¹ The definitions of $a_2, a_{3,5,7,9}$ are of the form: $a_2 = C_1 + C_2/3$, $a_i = C_i + C_{i+1}/3$ for $i = (3, 5, 7, 9)$.

TABLE I: The decay constants of $\psi(2S)$ meson is from [49], while other parameters are adopted in PDG [55] in our numerical calculations.

Mass(GeV)	$M_W = 80.385$	$M_B = 5.28$	$M_{B_s} = 5.37$	$m_b = 4.66$	$m_c = 1.275$
	$m_{\psi(2S)} = 3.686$	$m_\rho = 0.775$	$m_\omega = 0.783$	$m_{K^*} = 0.892$	$m_\phi = 1.019$
The Wolfenstein parameters	$\lambda = 0.22506,$		$A = 0.811,$	$\bar{\rho} = 0.124,$	$\bar{\eta} = 0.356$
Decay constants(MeV)	$f_B = 190.9 \pm 4.1$		$f_{B_s} = 227.2 \pm 3.4$	$f_{\psi(2S)} = 296_{-2}^{+3}$	
Lifetime(ps)	$\tau_{B_s} = 1.51$		$\tau_{B_0} = 1.52$	$\tau_{B^+} = 1.638$	

amplitudes in Eq. (6):

$$\begin{aligned}
 a_2 &\rightarrow a_2 + \frac{\alpha_s}{9\pi} C_2 \left[-18 - 12 \ln\left(\frac{\mu}{m_b}\right) + f_I^h \right], \\
 a_3 + a_9 &\rightarrow a_3 + a_9 + \frac{\alpha_s}{9\pi} (C_4 + C_{10}) \left[-18 - 12 \ln\left(\frac{\mu}{m_b}\right) + f_I^h \right], \\
 a_5 + a_7 &\rightarrow a_5 + a_7 + \frac{\alpha_s}{9\pi} (C_6 + C_8) \left[6 + 12 \ln\left(\frac{\mu}{m_b}\right) - f_I^h \right].
 \end{aligned} \tag{7}$$

The functions f_I^h arise from the vertex corrections, which are given in Ref. [31].

III. NUMERICAL RESULTS

To be used in our numerical calculations, those parameters such as meson mass, the Wolfenstein parameters, decay constants, and the lifetime of $B_{(s)}$ mesons [55] are given in Table I, while the input wave functions and various parameters of the light vectors are shown in Appendix B. We now use the method previously illustrated to estimate the physical observables (such as the CP averaged branching ratios, direct and mixing CP violations, polarization fractions, and relative phases) of the considered decays.

A. The CP averaged branching ratios

For $B \rightarrow \psi(2S)V$ decays, the branching ratios can be written as

$$\mathcal{B}(B \rightarrow \psi(2S)V) = \frac{G_F^2 \tau_B}{32\pi M} (1 - r^2) \sum_{i=0,\parallel,\perp} |\mathcal{A}_i|^2, \tag{8}$$

where the terms $\mathcal{A}_0, \mathcal{A}_\parallel, \mathcal{A}_\perp$ denote the longitudinal, parallel, and perpendicular polarization amplitude in the trasversity basis, respectively, which are related to $\mathcal{A}_{L,N,T}$ of Eq. (6) via

$$\mathcal{A}_0 = -\mathcal{A}_L, \quad \mathcal{A}_\parallel = \sqrt{2}\mathcal{A}_N, \quad \mathcal{A}_\perp = \sqrt{2}\mathcal{A}_T. \tag{9}$$

Here \mathcal{A}_0 and \mathcal{A}_\parallel are the CP even amplitudes whereas \mathcal{A}_\perp correspond to CP odd ones. Note that an additional minus sign in \mathcal{A}_0 (see Ref. [56]) make our definitions of the relative phase between $\mathcal{A}_{\parallel(\perp)}$ and \mathcal{A}_0 takes the value of π in the heavy-quark limit. The CP averaged branching ratios for the $B \rightarrow \psi(2S)V$ decays are shown in Table II together with some of the experimental measurements. Some dominant uncertainties are considered in our calculations. The first error in these entries is caused by the hadronic parameters in the $B_{(s)}$ meson wave function: (1) the shape parameters: $\omega_b = 0.40 \pm 0.04$ for the B meson, and $\omega_b = 0.50 \pm 0.05$ for the B_s meson; (2) the decay constants, which are given in Table I. The second error is from the uncertainty of the heavy quark masses. In the evaluation, we vary the values of $m_{c(b)}$ within a 10% range. The last one is caused by the variation of the hard scale from $0.8t$ to $1.2t$, which characterizes the size of the NLO QCD contributions. It is found that the main uncertainties in our approach come from the B meson wave function, which can reach 20 – 30% in magnitude. The scale-dependent uncertainty is less than 20% due to the inclusion of the NLO vertex corrections. We have checked the sensitivity of our results to the choice of the shape parameter ω_c (see Eq. (B7)) in charmonia meson wave function. The variation of ω_c in the

TABLE II: The PQCD predictions for the CP-averaged branching ratios for the $B \rightarrow \psi(2S)V$ decays (in units of 10^{-5}). For comparison, experimental results from BaBar [17], Belle [57, 58], or the world average from HFAG 2016 [59] and PDG 2016 [55] are also listed.

Modes	This work	BaBar [17]	Belle [57]	Belle [58]	HFAG 2016 [59]	PDG 2016 [55]
$B_s^0 \rightarrow \psi(2S)\bar{K}^{*0}$	$2.2^{+0.6+0.2+0.3}_{-0.5-0.2-0.2}$	–	–	–	–	3.3 ± 0.5
$B_s^0 \rightarrow \psi(2S)\phi$	$47^{+15+7+8}_{-10-3-4}$	–	–	–	–	54 ± 5
$B^+ \rightarrow \psi(2S)K^{*+}$	$59^{+14+7+7}_{-12-7-5}$	59.2 ± 12.3	81.3 ± 11.8	–	70.7 ± 8.5	67 ± 1.4
$B^0 \rightarrow \psi(2S)K^{*0}$	$54^{+13+6+7}_{-11-6-5}$	64.9 ± 11.4	72 ± 7.8	$55.5^{+4.7}_{-8.7}$	71.1 ± 6.2	59 ± 4
$B^+ \rightarrow \psi(2S)\rho^+$	$2.7^{+0.6+0.3+0.3}_{-0.6-0.3-0.2}$	–	–	–	–	–
$B^0 \rightarrow \psi(2S)\rho^0$	$1.2^{+0.3+0.1+0.1}_{-0.3-0.1-0.1}$	–	–	–	–	–
$B^0 \rightarrow \psi(2S)\omega$	$1.0^{+0.2+0.1+0.1}_{-0.2-0.1-0.1}$	–	–	–	–	–

range $0.18 \sim 0.22$ will result in a small change of the branching ratio, say less than 10%. In addition, the uncertainties related to the light vector mesons, such as the vector meson decay constants and the Gegenbauer moments shown in Table VI, are only several percent. Therefore they have been neglected in our calculations.

For the color-suppressed decays, it is expected that the factorizable diagram contribution is suppressed due to the cancellation of Wilson coefficients $C_1 + C_2/3$. After the inclusion of the vertex corrections, the factorizable diagram contributions become comparable with the nonfactorizable ones. Some important features of the numerical results collected in Table II are of the form

- (I) The $b \rightarrow s$ transition processes $B^{+(0)} \rightarrow \psi(2S)K^{*+(0)}$ and $B_s \rightarrow \psi(2S)\phi$ have a comparatively large branching ratio 10^{-4} ; while the branching ratios of those $b \rightarrow d$ channels $B^{+(0)} \rightarrow \psi(2S)\rho^{+(0)}$, $B^0 \rightarrow \psi(2S)\omega^0$ and $B_s \rightarrow \psi(2S)\bar{K}^{*0}$ are relatively small ($\sim 10^{-5}$) owing to the CKM factor suppression: $|V_{cb}^*V_{cd}| \sim \lambda^3$.
- (II) In the quark model, the difference between $B^0 \rightarrow \psi(2S)\omega$ and $B^0 \rightarrow \psi(2S)\rho^0$ decays comes from the sign of $d\bar{d}$ component, which only appears in penguin operators, so their difference should be relatively small. The branching ratio $\mathcal{B}(B^0 \rightarrow \psi(2S)\omega)$ is indeed slightly smaller than $\mathcal{B}(B^0 \rightarrow \psi(2S)\rho^0)$. This is a consequence of the fact that the ω vector and tensor decay constants are smaller than those of the ρ^0 according to Table VI;
- (III) The value of $\mathcal{B}(B_s \rightarrow \psi(2S)\bar{K}^{*0})$ have a tendency to be smaller than $2\mathcal{B}(B^0 \rightarrow \psi(2S)\rho^0)$. Although the K^* and B_s meson decay constants are larger than those of the ρ^0 and B^0 meson, the SU(3) breaking effects in the twist-2 distribution amplitudes, parametrized by the first Gegenbauer moment a_{1K^*} (see Eq. (B10)), gives a negative contribution to the $B_s \rightarrow \psi(2S)\bar{K}^{*0}$ decay, which induces the smaller branching ratio.
- (IV) For the first four $B_{(s)} \rightarrow \psi(2S)V$ decays as listed in Table II, one can see that the PQCD predictions for their branching ratios agree well with the world averaged values as given in HFAG 2016 and PDG 2016 [55, 59] within one standard deviation. For $B_s \rightarrow \psi(2S)\bar{K}^{*0}$ decay, the central value of our theoretical prediction for its branching ratio is slightly smaller than that of the PDG number [55]. But we know that the PDG result is obtained by multiplying the best value $\mathcal{B}(B^0 \rightarrow \psi(2S)K^{*0})$ with the measured ratio $\mathcal{B}(\bar{B}_s^0 \rightarrow \psi(2S)K^{*0})/\mathcal{B}(B^0 \rightarrow \psi(2S)K^{*0})$ from the LHCb [60]. We hope the future experiment will provide a direct measurement to this mode.
- (V) As for the channels with ρ and ω as the final state V meson, they have not been measured yet. The pQCD predictions for the decay rates of these three channels are at the order of 10^{-5} , measurable in the future LHCb and Belle-II experiments.

For a more direct comparison with the available experimental measurements of the relative rates of $B_{(s)}$ meson decays into $\psi(2S)$ and J/ψ mesons, we recalculated the corresponding $B_{(s)}$ decays to $J/\psi V$ by using the same input

parameters as in this paper but with the replacement $\psi(2S) \rightarrow J/\psi$, and we found numerically that

$$\begin{aligned}
\mathcal{B}(B_s \rightarrow J/\psi \bar{K}^{*0}) &= (4.2_{-0.8-0.3-0.1}^{+1.2+0.6+0.6}) \times 10^{-5}, \\
\mathcal{B}(B_s \rightarrow J/\psi \phi) &= (9.3_{-1.9-0.7-0.8}^{+2.6+1.0+1.5}) \times 10^{-4}, \\
\mathcal{B}(B^+ \rightarrow J/\psi K^{*+}) &= (11.2_{-2.2-1.2-0.9}^{+2.5+1.4+1.5}) \times 10^{-4}, \\
\mathcal{B}(B^0 \rightarrow J/\psi K^{*0}) &= (10.4_{-2.0-1.1-0.8}^{+2.2+1.3+1.3}) \times 10^{-4}, \\
\mathcal{B}(B^+ \rightarrow J/\psi \rho^+) &= (5.1_{-1.0-0.5-0.3}^{+1.2+0.6+0.8}) \times 10^{-5}, \\
\mathcal{B}(B^0 \rightarrow J/\psi \rho^0) &= (2.4_{-0.5-0.3-0.2}^{+0.6+0.3+0.4}) \times 10^{-5}, \\
\mathcal{B}(B^0 \rightarrow J/\psi \omega) &= (1.8_{-0.4-0.1-0.1}^{+0.4+0.2+0.3}) \times 10^{-5},
\end{aligned} \tag{10}$$

where the errors have the same meaning as those for $B_{(s)} \rightarrow \psi(2S)V$ decays. The above results are well consistent with the previous PQCD calculations [52] and also the present data [55].

Finally, as a cross-check, using the PQCD predictions as given in Table II and Eq. (10) we can estimate the relative ratios $\mathcal{R}_V = \mathcal{B}(B \rightarrow \psi(2S)V)/\mathcal{B}(B \rightarrow J/\psi V)$ as below,

$$\begin{aligned}
\mathcal{R}_\phi &= 0.51_{-0.01}^{+0.02}, & \mathcal{R}_{K^{*0(+)}} &= 0.53_{-0.02}^{+0.00}, & \mathcal{R}_{\rho^{0(+)}} &= 0.53_{-0.03}^{+0.00}, \\
\mathcal{R}_\omega &= 0.56_{-0.04}^{+0.01}, & \mathcal{R}_{\bar{K}^{*0}} &= 0.52_{-0.04}^{+0.01},
\end{aligned} \tag{11}$$

where all uncertainties are added in quadrature. Since the parameter dependences of the PQCD predictions for the branching ratios are largely canceled in their relative ratios, the total theoretical error of R_V are only a few percent, much smaller than those for the branching ratios. Fortunately, two of these five ratios have been measured by LHCb [24] D0 [25], and CDF [14, 26] experiments:

$$\begin{aligned}
\mathcal{R}_\phi &= \begin{cases} 0.489 \pm 0.026(\text{stat}) \pm 0.021(\text{syst}) \pm 0.012(R_\psi) & \text{LHCb} \\ 0.53 \pm 0.10(\text{stat}) \pm 0.07(\text{syst}) \pm 0.06(R_\psi) & \text{D0} \\ 0.52 \pm 0.13(\text{stat}) \pm 0.04(\text{syst}) \pm 0.06(R_\psi) & \text{CDF} \end{cases} \\
\mathcal{R}_{K^{*0}} &= \begin{cases} 0.476 \pm 0.014(\text{stat}) \pm 0.010(\text{syst}) \pm 0.012(R_\psi) & \text{LHCb} \\ 0.515 \pm 0.113(\text{stat}) \pm 0.052(\text{syst}) & \text{CDF} \end{cases},
\end{aligned} \tag{12}$$

where the third uncertainty is from the ratio of the $\psi(2S)$ and J/ψ branching fractions to $\mu^+\mu^-$. It is easy to see that our PQCD predictions for both R_ϕ and $R_{K^{*0}}$ agree very well with the measured values.

B. CP ASYMMETRIES

Studying CP asymmetries is an important task in B physics. For the charged B decays, the CP asymmetries arise from the interference between the penguin diagrams and tree diagrams. The direct CP violation asymmetry including three polarization are defined by

$$A_{0,\parallel,\perp}^{\text{dir}} = \frac{|\bar{\mathcal{A}}_{0,\parallel,\perp}|^2 - |\mathcal{A}_{0,\parallel,\perp}|^2}{|\bar{\mathcal{A}}_{0,\parallel,\perp}|^2 + |\mathcal{A}_{0,\parallel,\perp}|^2}, \tag{13}$$

where $\bar{\mathcal{A}}_{0,\parallel,\perp}$ is the CP -conjugate amplitude of $\mathcal{A}_{0,\parallel,\perp}$.

For the neutral $B_{(s)}^0$ decays, because of the $B_{(s)}^0 - \bar{B}_{(s)}^0$ mixing, it is required to include time-dependent measurements in CP violation asymmetries. If the final states are CP eigen states, the time-dependent CP asymmetry is defined as

$$A_f^{0,\parallel,\perp}(t) = -C_f^{0,\parallel,\perp} \cos(\Delta m t) + S_f^{0,\parallel,\perp} \sin(\Delta m t), \tag{14}$$

where Δm is the mass difference of the two mass eigenstates of the neutral B meson and f is a two-body final state. The direct CP asymmetry $C_f^{0,\parallel,\perp}$ and mixing-induced CP asymmetry $S_f^{0,\parallel,\perp}$ are referred to as

$$C_f^{0,\parallel,\perp} = \frac{1 - |\lambda_f^{0,\parallel,\perp}|^2}{1 + |\lambda_f^{0,\parallel,\perp}|^2}, \quad S_f = \frac{2\text{Im}(\lambda_f^{0,\parallel,\perp})}{1 + |\lambda_f^{0,\parallel,\perp}|^2}. \tag{15}$$

TABLE III: The PQCD predictions for $A_{0,\parallel,\perp}^{\text{dir}}(10^{-3})$ in the $B \rightarrow \psi(2S)(\rho^+, K^*, \bar{K}^*)$ decays. The error arises from the hard scale t .

Modes	A_0^{dir}	$A_{\parallel}^{\text{dir}}$	A_{\perp}^{dir}	A^{dir}
$B^+ \rightarrow \psi(2S)\rho^+$	$-5.9^{+6.6}_{-11.9}$	$-8.3^{+6.9}_{-7.0}$	$-9.2^{+5.7}_{-11.3}$	$-7.2^{+6.6}_{-10.5}$
$B^+ \rightarrow \psi(2S)K^{*+}$	$0.4^{+0.6}_{-0.4}$	$0.4^{+1.3}_{-0.4}$	$0.5^{+0.3}_{-0.3}$	$0.4^{+0.8}_{-0.4}$
$B_s^0 \rightarrow \psi(2S)\bar{K}^{*0}$	$-5.2^{+7.2}_{-9.2}$	$-5.7^{+6.7}_{-7.0}$	$-7.1^{+5.7}_{-9.4}$	$-5.7^{+5.8}_{-8.7}$
$B^0 \rightarrow \psi(2S)K^{*0}$	$0.4^{+0.6}_{-0.4}$	$0.4^{+1.3}_{-0.4}$	$0.5^{+0.3}_{-0.3}$	$0.4^{+0.8}_{-0.4}$

TABLE IV: The PQCD predictions for the CP asymmetry parameters $C_f^{0,\parallel,\perp}$ and $S_f^{0,\parallel,\perp}$ in the $B^0 \rightarrow \psi(2S)(\rho^0, \omega, \phi)$ decays. The error arises from the hard scale t .

Modes	$C_f^0(10^{-3})$	S_f^0	$C_f^{\parallel}(10^{-3})$	S_f^{\parallel}	$C_f^{\perp}(10^{-3})$	S_f^{\perp}
$B^0 \rightarrow \psi(2S)\rho^0$	$5.9^{+11.2}_{-6.7}$	$-0.68^{+0.00}_{-0.01}$	$8.3^{+6.6}_{-5.9}$	$-0.69^{+0.00}_{-0.00}$	$9.2^{+11.8}_{-6.1}$	$0.69^{+0.01}_{-0.00}$
$B^0 \rightarrow \psi(2S)\omega$	$6.4^{+7.7}_{-6.0}$	$-0.68^{+0.00}_{-0.01}$	$7.9^{+8.9}_{-6.7}$	$-0.69^{+0.00}_{-0.01}$	$8.9^{+10.2}_{-5.7}$	$0.69^{+0.01}_{-0.00}$
$B_s^0 \rightarrow \psi(2S)\phi$	$-0.4^{+0.3}_{-0.4}$	$-0.038^{+0.001}_{-0.000}$	$-0.3^{+0.2}_{-0.5}$	$-0.038^{+0.001}_{-0.000}$	$-0.4^{+0.3}_{-0.3}$	$0.037^{+0.000}_{-0.001}$

The parameter $\lambda_f^{0,\parallel,\perp} = \eta_f e^{-2i\beta_{(s)}} \frac{\bar{\mathcal{A}}_{0,\parallel,\perp}}{\mathcal{A}_{0,\parallel,\perp}}$ describes CP violation in the interference between mixing and decay. η_f is the CP eigenvalue (± 1) of the polarization state. $\beta_{(s)}$ is the CKM angle defined as usual [55]. Note that the final states of $\psi(2S)K^{*0}$ and its CP conjugate are flavor-specific, for example, the kaon and pion charges of $K^{*0} \rightarrow K^+\pi^-$ and $\bar{K}^{*0} \rightarrow K^-\pi^+$ depend on whether we had a B and \bar{B} meson in the initial state, and the time-dependent angular distributions do not show CP violation due to interference between mixing and decay. Therefore, we only calculate the direct CP asymmetry for $B_s^0 \rightarrow \psi(2S)\bar{K}^{*0}$ and $B^0 \rightarrow \psi(2S)K^{*0}$ decays.

The PQCD predictions for the CP asymmetry parameters $A_{0,\parallel,\perp}^{\text{dir}}$ are listed in Table III and IV. Unlike the branching ratios, the direct CP asymmetry is not sensitive to the wave function parameters and heavy quark masses, but suffer from large uncertainties due to the hard scale t . In order to reduce the large scale dependence effectively, one has to know the complete NLO corrections, which are in fact not yet available now, thus beyond the scope of this paper.

Since the direct CP asymmetry is proportional to the interference between the tree and penguin contributions, while the Wilson coefficients of the penguin diagram are loop suppressed when compared with those tree contributions. Therefore, the direct CP asymmetry parameters of these processes are rather small (only $10^{-3} \sim 10^{-4}$), and the mixing-induced CP asymmetry for neutral B decays is almost proportional to the $\sin 2\beta_{(s)}$ from Eq. (15). The mixing-induced CP asymmetry parameters $S_{\psi(2S)\rho^0(\omega)}$ and $S_{\psi(2S)\phi}$ in Table IV are very close to the current world average values $-\sin 2\beta = -0.691 \pm 0.017$ and $-2\beta_s = -0.0376^{+0.0008}_{-0.0007}$ [59], respectively. That is to say, these modes can serve as an alternative places to extract CKM angle $\beta_{(s)}$. Furthermore, the large mixing-induced CP asymmetry S_f for $b \rightarrow d$ transition can confront with future experimental results. It can also be seen that the CP asymmetry parameters for three polarization states are slightly different because the strong phases coming from the non-factorizable diagrams and vertex corrections are polarization-dependent [31]. On experimental side, so far only the charge asymmetries of $B^+ \rightarrow \psi(2S)K^{*+}$ process was measured by BaBar Collaboration [55]:

$$A_{CP}^{\text{dir}}(B^+ \rightarrow \psi(2S)K^{*+}) = 0.08 \pm 0.21. \quad (16)$$

Of course, the statistical uncertainty is too large to make any statement. Any observation of large direct CP asymmetry for the considered decays $B_{(s)} \rightarrow \psi(2S)V$ decays will be a signal for new physics. Besides, the precise measurements of these mixing-induced CP asymmetries serve to determine the CP phases related to the $B^0 - \bar{B}^0$ and $B_s^0 - \bar{B}_s^0$ mixing amplitudes.

C. Polarization fractions and relative phases

In experimental analyses, we usually define five observables corresponding to three polarization fractions $f_0, f_{\parallel}, f_{\perp}$, and two relative phases $\phi_{\parallel}, \phi_{\perp}$, where

$$f_{0,\parallel,\perp} = \frac{|\mathcal{A}_{0,\parallel,\perp}|^2}{|\mathcal{A}_0|^2 + |\mathcal{A}_{\parallel}|^2 + |\mathcal{A}_{\perp}|^2}, \quad \phi_{\parallel,\perp} = \arg \frac{\mathcal{A}_{\parallel,\perp}}{\mathcal{A}_0}, \quad (17)$$

TABLE V: The PQCD predictions for the CP-averaged polarization fractions, relative phases in the $B \rightarrow \psi(2S)V$ decays. The errors correspond to the combined uncertainty in the hadronic parameters, heavy quark masses and the hard scale t .

Modes	f_0	f_{\parallel}	f_{\perp}	$\phi_{\parallel}(\text{rad})$	$\phi_{\perp}(\text{rad})$
$B^+ \rightarrow \psi(2S)K^{*+}$	$0.48^{+0.01+0.07+0.01}_{-0.02-0.08-0.01}$	$0.28^{+0.01+0.03+0.00}_{-0.00-0.03-0.00}$	$0.24^{+0.01+0.05+0.00}_{-0.00-0.05-0.00}$	$2.43^{+0.01+0.09+0.03}_{-0.02-0.09-0.04}$	$2.15^{+0.02+0.16+0.01}_{-0.03-0.16-0.05}$
CLEO [15]	$0.51 \pm 0.16 \pm 0.05$	–	–	–	–
$B^0 \rightarrow \psi(2S)K^{*0}$	$0.48^{+0.01+0.07+0.01}_{-0.02-0.08-0.01}$	$0.28^{+0.01+0.03+0.00}_{-0.00-0.03-0.00}$	$0.24^{+0.01+0.05+0.00}_{-0.00-0.05-0.00}$	$2.43^{+0.01+0.09+0.03}_{-0.02-0.09-0.04}$	$2.15^{+0.02+0.16+0.01}_{-0.03-0.16-0.05}$
BaBar [18]	$0.48 \pm 0.05 \pm 0.02$	$0.22 \pm 0.06 \pm 0.02$	$0.30 \pm 0.06 \pm 0.02$	$3.5 \pm 0.4 \pm 0.1^a$	$2.8 \pm 0.3 \pm 0.1$
CLEO [15]	$0.40 \pm 0.14 \pm 0.07$	–	–	–	–
Belle [58]	$0.455^{+0.031+0.014}_{-0.029-0.049}$	–	–	–	–
$B_s^0 \rightarrow \psi(2S)\bar{K}^{*0}$	$0.50^{+0.01+0.06+0.01}_{-0.02-0.07-0.01}$	$0.28^{+0.00+0.02+0.00}_{-0.00-0.04-0.01}$	$0.23^{+0.01+0.04+0.00}_{-0.01-0.04-0.01}$	$2.48^{+0.01+0.08+0.02}_{-0.02-0.08-0.04}$	$2.20^{+0.03+0.16+0.05}_{-0.02-0.13-0.05}$
LHCb [60]	$0.524 \pm 0.056 \pm 0.029$	–	–	–	–
$B_s^0 \rightarrow \psi(2S)\phi$	$0.48^{+0.01+0.05+0.00}_{-0.02-0.06-0.01}$	$0.29^{+0.00+0.02+0.00}_{-0.01-0.03-0.01}$	$0.24^{+0.00+0.04+0.00}_{-0.01-0.04-0.01}$	$2.59^{+0.01+0.08+0.02}_{-0.01-0.05-0.03}$	$2.31^{+0.02+0.14+0.03}_{-0.04-0.11-0.04}$
LHCb [13]	$0.422 \pm 0.014 \pm 0.003$	–	$0.264^{+0.024}_{-0.023} \pm 0.002$	$3.67^{+0.13}_{-0.18} \pm 0.03$	$3.29^{+0.43}_{-0.39} \pm 0.04$
$B^+ \rightarrow \psi(2S)\rho^+$	$0.54^{+0.01+0.06+0.01}_{-0.02-0.08-0.00}$	$0.25^{+0.01+0.03+0.01}_{-0.01-0.03-0.01}$	$0.21^{+0.01+0.05+0.00}_{-0.01-0.04-0.00}$	$2.32^{+0.02+0.12+0.03}_{-0.02-0.12-0.03}$	$2.05^{+0.02+0.17+0.04}_{-0.04-0.20-0.06}$
$B^0 \rightarrow \psi(2S)\rho^0$	$0.54^{+0.01+0.06+0.01}_{-0.02-0.08-0.00}$	$0.25^{+0.01+0.03+0.01}_{-0.01-0.03-0.01}$	$0.21^{+0.01+0.05+0.00}_{-0.01-0.04-0.00}$	$2.32^{+0.02+0.12+0.03}_{-0.02-0.12-0.03}$	$2.05^{+0.02+0.17+0.04}_{-0.04-0.20-0.06}$
$B^0 \rightarrow \psi(2S)\omega^0$	$0.52^{+0.02+0.08+0.01}_{-0.01-0.07-0.00}$	$0.25^{+0.01+0.03+0.01}_{-0.00-0.02-0.00}$	$0.22^{+0.01+0.05+0.00}_{-0.01-0.04-0.01}$	$2.34^{+0.02+0.11+0.05}_{-0.02-0.12-0.03}$	$2.07^{+0.02+0.17+0.04}_{-0.03-0.19-0.06}$

^aWe choose the equivalent solution in $(0, 2\pi)$

with normalisation such that $f_0 + f_{\parallel} + f_{\perp} = 1$. The polarization fractions as well as relative phases are shown in Table V, where the sources of the errors in the numerical estimates have the same origin as in the discussion of the branching ratios in Table II. It is easy to see that the most important theoretical uncertainties are caused by the heavy quark masses. From Eqs. (7) and (A10), we can see the mass terms m_b and m_c associated vertex corrections and nonfactorizable amplitudes, respectively. It can numerically change the real and imaginary parts of these contributions and have a significant effect on the polarization fractions, especially for the relative phases. The uncertainties from the wave function parameters are very small because they mainly give an overall change of all polarization amplitudes and the parameter dependence can be canceled out in Eq. (17).

From Table V, both the $B^+ \rightarrow \psi(2S)(K^{*+}, \rho^+)$ and $B^0 \rightarrow \psi(2S)(K^{*0}, \rho^0)$ modes have the same polarization fractions and relative phases, since they differ only in the lifetimes or isospin factor in our formalism. Comparing the three polarization fractions, the perpendicular polarization fractions f_{\perp} are less than 25% shows that the CP even component dominates in these decays. According to the power counting rules in the factorization assumption, the longitudinal polarization dominates the decay ratios and the transverse polarizations are suppressed [61] due to the helicity flips of the quark in the final state hadrons. However, the situation is very different for the color-suppressed decays, where the contributions from the nonfactorizable tree diagrams in Figs. 1(c) and 1(d) are comparable with those of the color-suppressed tree diagrams although the latter are enhanced by the involving vertex corrections. With an additional gluon, the transverse polarization in the nonfactorizable diagrams does not encounter helicity flip suppression, therefore numerically we get a longitudinal polarization fraction (f_0) smaller than 50%, which are compatible with those currently available data. The fact that the nonfactorizable diagrams can give a large transverse polarization contribution is also observed in the $B_c \rightarrow J/\psi D_{(s)}^{*+}$ decays [62]. There are another equivalent set of helicity amplitudes ($\mathcal{A}_0, \mathcal{A}_+, \mathcal{A}_-$), which are related to the spin amplitudes ($\mathcal{A}_0, \mathcal{A}_{\parallel}, \mathcal{A}_{\perp}$) introduced in Eq. (9) by

$$\mathcal{A}_{\pm} = \frac{\mathcal{A}_{\parallel} \pm \mathcal{A}_{\perp}}{\sqrt{2}}, \quad (18)$$

while \mathcal{A}_0 is common to both bases.

It is expected that $|\mathcal{A}_0|^2 > |\mathcal{A}_+|^2 > |\mathcal{A}_-|^2$ if the two final-states are both light vector mesons. The larger the mass of the vector-meson daughters, the weaker the inequality. In $B \rightarrow \psi(2S)V$ decays with light V being a recoiled meson and heavy $\psi(2S)$ an ejected one. The positive-helicity amplitude is suppressed by $m_{\psi(2S)}/M$ (almost of order unity) due to one of the quark helicities in $\psi(2S)$ has to be flipped, while the negative-helicity one is subject to a further chirality suppression of order m_V/M [61]. Therefore, \mathcal{A}_+ and \mathcal{A}_0 can be comparable and larger than \mathcal{A}_- . Using values of Table V and Eq. (18), the pQCD predictions do favor the hierarchy pattern $|\mathcal{A}_0|^2 \sim |\mathcal{A}_+|^2 > |\mathcal{A}_-|^2$.

The angular analysis of $B^0 \rightarrow \psi(2S)K^{*0}$ and $B_s^0 \rightarrow \psi(2S)\phi$ has been carried out by BaBar [18] and LHCb [13], respectively. The obtained polarization observables are also summarized in Table V. As expected under $SU(3)$ -flavor symmetry, both decay modes have similar magnitudes and phases of the amplitudes. Our results of polarization fractions can accommodate the data well within uncertainties, while the predicted relative phases are a bit smaller

than the data. One can find a shift from π at the $6-7\sigma$ level in ϕ_{\parallel} and ϕ_{\perp} shows the existence of final-state interaction. However, the $f_{\parallel} - f_{\perp}$ is about 5% and the difference between ϕ_{\parallel} and ϕ_{\perp} dose not exceed 0.3 radians, which suggest that our solutions are consistent with approximate s-quark helicity conservation despite substantial strong phases.

For the $B_s^0 \rightarrow \psi(2S)\bar{K}^{*0}$ channel, the LHCb Collaboration [60] has reported the longitudinal polarisation fraction f_0 as $0.524 \pm 0.056 \pm 0.029$, but a thorough angular analysis is still missing. As for other modes, we obtain reasonably accurate results, which could be tested by future experimental measurements.

IV. CONCLUSION

In this paper we have investigated the seven $B \rightarrow \psi(2S)V$ decay modes carefully by employing the PQCD factorization approach. Besides the color-suppressed factorizable diagrams, the nonfactorizable diagrams and the vertex correction diagrams can also be evaluated in this approach.

The predicted branching ratios and the relative rates of B meson decays into $\psi(2S)$ and J/ψ mesons are compared with experiments wherever available. Our results indicate that the direct CP asymmetries in these channels are very small due to the suppressed penguin contributions as we mentioned above. The mixing-induced CP asymmetries are not far away from $\sin 2\beta_{(s)}$, these channels can therefore play an important role in the extraction of the CKM angle $\beta_{(s)}$.

Finally, we made a comprehensive polarization analysis of the considered decays. The predicted polarization fractions and relative phases of $B^0 \rightarrow \psi(2S)K^{*0}$ and $B_s^0 \rightarrow \psi(2S)\phi$ decays are consistent with data. Due to the large mass of $\psi(2S)$ and the dominant contributions from the nonfactorizable diagrams, we obtain an equal amount of transverse and longitudinal polarization. The pattern of $f_{\parallel} \approx f_{\perp}$, $\phi_{\parallel} \approx \phi_{\perp}$ favor the conservation of light quark helicity. The deviations from π at several standard deviations in ϕ_{\parallel} and ϕ_{\perp} indicate the existence of the still unknown final-state interaction.

We also discussed theoretical uncertainties arising from the hadronic parameters in B meson wave function, heavy quark masses and hard scale t . The total uncertainties are acceptable, around 30% in magnitude. The uncertainties from the hadronic parameters can give sizable effects on the PQCD predictions for branching ratios, while the CP asymmetries suffer a large error from the hard scale t . The further studies at the completely NLO level are certainly required to improve the accuracy of the theoretical predictions. Furthermore, the polarization observables $f_{0,\parallel,\perp}$ and $\phi_{\parallel,\perp}$ are more sensitive to the heavy quark masses, which suggest that the color-suppressed type decays may be more sensitive to the vertex corrections and nonfactorizable contributions. Our results and findings will be further tested by the LHCb and Belle-II experiments in the near future.

Acknowledgments

The authors are grateful to Hsiang-nan Li for helpful discussions. This work is supported in part by National Natural Science Foundation of China under Grants Nos. 11547020, 11605060, and 11235005, in part by Natural Science Foundation of Hebei Province under Grant No. A2014209308, in part by Program for the Top Young Innovative Talents of Higher Learning Institutions of Hebei Educational Committee under Grant No. BJ2016041, and in part by Training Foundation of North China University of Science and Technology under Grant No. GP201520 and No. JP201512.

Appendix A: THE DECAY AMPLITUDES

Following the derivation of the factorization formula of Eq. (2), we get the analytic formulas of the (non)factorizable amplitude for each helicity state listed below.

$$\begin{aligned}
\mathcal{F}_L^{LL} = & -8\pi C_f f_{\psi} M^4 \int_0^1 dx_1 dx_3 \int_0^{\infty} b_1 b_3 db_1 db_3 \phi_B(x_1, b_1) \\
& \{ \sqrt{1-r^2} [\phi_V(x_3)((r^2-1)x_3-1) + \phi_V^s(x_3)\sqrt{1-r^2}r_v(2x_3-1) + \\
& \phi_V^t(x_3)r_v(2x_3-1-r^2(1+2x_3))] \alpha_s(t_a) S_{ab}(t_a) h(\alpha_e, \beta_a, b_1, b_3) S_t(x_1) \\
& - 2r_v(1-r^2)\phi_V^s(x_3)\alpha_s(t_b) S_{ab}(t_b) h(\alpha_e, \beta_b, b_1, b_3) S_t(x_3) \}, \tag{A1}
\end{aligned}$$

$$\begin{aligned}
\mathcal{F}_N^{LL} &= 8\pi C_f f_\psi M^4 r \int_0^1 dx_1 dx_3 \int_0^\infty b_1 b_3 db_1 db_3 \phi_B(x_1, b_1) \\
&\quad \{[(r^2 - 1)(\phi_V^a(x_3)r_v x_3 - \phi_V^T(x_3)) + r_v \phi_V^v(2 + (1 - r^2)x_3)]\alpha_s(t_a) S_{ab}(t_a) h(\alpha_e, \beta_a, b_1, b_3) S_t(x_1) \\
&\quad + r_v(1 - r^2)(\phi_V^a(x_3) + \phi_V^v(x_3))\alpha_s(t_b) S_{ab}(t_b) h(\alpha_e, \beta_b, b_1, b_3) S_t(x_3)\}, \tag{A2}
\end{aligned}$$

$$\mathcal{F}_T^{LL} = \mathcal{F}_N^{LL} |_{\phi_V^a \leftrightarrow \phi_V^v}, \tag{A3}$$

$$\mathcal{F}_{L,N,T}^{LR} = \mathcal{F}_{L,N,T}^{LL}, \tag{A4}$$

$$\begin{aligned}
\mathcal{M}_L^{LL} &= -16\sqrt{\frac{2}{3}}\pi C_f M^4 \int_0^1 dx_1 dx_2 dx_3 \int_0^\infty b_1 b_2 db_1 db_2 \phi_B(x_1, b_1) \\
&\quad \{\sqrt{1 - r^2}[\psi^L(x_2, b_2)r_v(\phi_V^s(x_3)\sqrt{1 - r^2} + \phi_V^t(x_3)(r^2(2x_2 + x_3 - 2) - x_3)) \\
&\quad - \phi_V(x_3)(\psi^L(x_2, b_2)(r^2 - 1)(x_2 - 1) + \psi^t(x_2, b_2)r_c r)]\alpha_s(t_c) S_{cd}(t_c) h(\alpha_e, \beta_c, b_1, b_2) \\
&\quad + [\psi^L(x_2, b_2)(x_2(\phi_V(x_3)(r^2 + 1) - 2r^2 r_v \phi_V^t(x_3)) - (r^2 - 1)x_3(\phi_V(x_3) - r_v \phi_V^t(x_3))) \\
&\quad - \phi_V^s(x_3)\sqrt{1 - r^2}r_v x_3 - \psi^t(x_2, b_2)r_c r(\phi_V(x_3) - 4r_v \phi_V^t(x_3))]\alpha_s(t_d) S_{cd}(t_d) h(\alpha_e, \beta_d, b_1, b_2)\}, \tag{A5}
\end{aligned}$$

$$\begin{aligned}
\mathcal{M}_N^{LL} &= 16\sqrt{\frac{2}{3}}\pi C_f M^4 \int_0^1 dx_1 dx_2 dx_3 \int_0^\infty b_1 b_2 db_1 db_2 \phi_B(x_1, b_1) \\
&\quad \{[(r^2 - 1)(r_c r_v \psi^T(x_2, b_2)\phi_V^a(x_3) + r(x_2 - 1)\psi^V(x_2, b_2)\phi_V^T(x_3)) \\
&\quad + \psi^T(x_2, b_2)\phi_V^v(x_3)r_c r_v(1 + r^2)]\alpha_s(t_c) S_{cd}(t_c) h(\alpha_e, \beta_c, b_1, b_2) \\
&\quad + [\phi_V^v(x_3)r_v(\psi^T(x_2, b_2)r_c(1 + r^2) - 2\psi^V(x_2, b_2)r(x_2(1 + r^2) + x_3(1 - r^2))) \\
&\quad - (r^2 - 1)(\phi_V^T(x_3)(\psi^V(x_2, b_2)r x_2 - 2\psi^T(x_2, b_2)r_c) + r_c r_v \phi_V^a(x_3)\psi^T(x_2, b_2))] \\
&\quad \alpha_s(t_d) S_{cd}(t_d) h(\alpha_e, \beta_d, b_1, b_2)\}, \tag{A6}
\end{aligned}$$

$$\mathcal{M}_T^{LL} = \mathcal{M}_N^{LL} |_{\phi_V^a \leftrightarrow \phi_V^v}, \tag{A7}$$

$$\mathcal{M}_{L,N,T}^{SP} = -\mathcal{M}_{L,N,T}^{LL}, \tag{A8}$$

with $r_c = m_c/M$ and m_c is the charm quark mass; $C_f = 4/3$ is a color factor; f_ψ is the decay constant of the $\psi(2S)$ meson. The coefficient $(-)\frac{1}{\sqrt{2}}$ appears for $B \rightarrow \psi(2S)(\rho^0)\omega$ decay, because only the d quark component of the $(\rho^0)\omega$ meson is involved. We neglect terms higher than r_v^2 orders, since the vector light cone wave functions derived from sum rules are expanded to this order [63]. The functions h come from the Fourier transform of virtual quark and gluon propagators. They are defined by

$$\begin{aligned}
h(\alpha, \beta, b_1, b_2) &= h_1(\alpha, b_1) \times h_2(\beta, b_1, b_2), \\
h_1(\alpha, b_1) &= \begin{cases} K_0(\sqrt{\alpha}b_1), & \alpha > 0, \\ K_0(i\sqrt{-\alpha}b_1), & \alpha < 0, \end{cases} \\
h_2(\beta, b_1, b_2) &= \begin{cases} \theta(b_1 - b_2)I_0(\sqrt{\beta}b_2)K_0(\sqrt{\beta}b_1) + (b_1 \leftrightarrow b_2), & \beta > 0, \\ \theta(b_1 - b_2)J_0(\sqrt{-\beta}b_2)K_0(i\sqrt{-\beta}b_1) + (b_1 \leftrightarrow b_2), & \beta < 0, \end{cases} \tag{A9}
\end{aligned}$$

where J_0 is the Bessel function and K_0, I_0 are modified Bessel function with $K_0(ix) = \frac{\pi}{2}(-N_0(x) + iJ_0(x))$. α_e and $\beta_{a,b,c,d}$ are the virtuality of the internal gluon and quark, respectively. Their expressions are

$$\begin{aligned}
\alpha_e &= x_1 x_3 (1 - r^2) M^2, \quad \beta_a = x_3 (1 - r^2) M^2, \quad \beta_b = x_1 (1 - r^2) M^2, \\
\beta_c &= [(x_1 + x_2 - 1)(x_3 + r^2(1 - x_2 - x_3)) + r_c^2] M^2, \\
\beta_d &= [(x_1 - x_2)(x_3 + r^2(x_2 - x_3)) + r_c^2] M^2. \tag{A10}
\end{aligned}$$

The hard scale t is chosen as the maximum of the virtuality of the internal momentum transition in the hard amplitudes, including $1/b_i (i = 1, 2, 3)$:

$$t_{a,b} = \max(\sqrt{\beta_{a,b}}, 1/b_1, 1/b_3), \quad t_{c,d} = \max(\sqrt{\alpha_e}, \sqrt{\beta_{c,d}}, 1/b_1, 1/b_2). \quad (\text{A11})$$

The Sudakov factors can be written as

$$\begin{aligned} S_{ab}(t) &= s\left(\frac{M_B}{\sqrt{2}}x_1, b_1\right) + s\left(\frac{M_B}{\sqrt{2}}x_3(1-r^2), b_3\right) + s\left(\frac{M_B}{\sqrt{2}}(1-x_3)(1-r^2), b_3\right) \\ &\quad + \frac{5}{3} \int_{1/b_1}^t \frac{d\mu}{\mu} \gamma_q(\mu) + 2 \int_{1/b_3}^t \frac{d\mu}{\mu} \gamma_q(\mu), \\ S_{cd}(t) &= s\left(\frac{M_B}{\sqrt{2}}x_1, b_1\right) + s\left(\frac{M_B}{\sqrt{2}}x_2, b_2\right) + s\left(\frac{M_B}{\sqrt{2}}(1-x_2), b_2\right) \\ &\quad + s\left(\frac{M_B}{\sqrt{2}}x_3(1-r^2), b_1\right) + s\left(\frac{M_B}{\sqrt{2}}(1-x_3)(1-r^2), b_1\right) \\ &\quad + \frac{11}{3} \int_{1/b_1}^t \frac{d\mu}{\mu} \gamma_q(\mu) + 2 \int_{1/b_2}^t \frac{d\mu}{\mu} \gamma_q(\mu), \end{aligned} \quad (\text{A12})$$

where the function $s(Q, b)$ is given in [64]. $\gamma_q = -\alpha_s/\pi$ is the anomalous dimension of the quark. The threshold resummation factor $S_t(x)$ is adopted from [65],

$$S_t(x) = \frac{2^{1+2c}\Gamma(3/2+c)}{\sqrt{\pi}\Gamma(1+c)} [x(1-x)]^c, \quad (\text{A13})$$

with a running parameter $c(Q^2) = 0.04Q^2 - 0.51Q + 1.87$ [66] and $Q^2 = M^2(1-r^2)$ [67].

Appendix B: THE WAVE FUNCTIONS

In the PQCD approach, the necessary inputs contain the light-cone distribution amplitudes (LCDAs) which are constructed by the nonlocal matrix elements. The $B_{u,d,s}$ meson light-cone matrix element are decomposed into the following two Lorentz structures [54]:

$$\int d^4z e^{ik_1 \cdot z} \langle 0 | q_\alpha(z) \bar{b}(0)_\beta | B_q(P_1) \rangle = \frac{i}{\sqrt{2N_c}} \{ (P_1 + M) \gamma_5 [\Phi_{B_q}(k_1) - \frac{\not{t} - \not{t}'}{\sqrt{2}} \bar{\Phi}_{B_q}(k_1)] \}_{\alpha\beta}, \quad (\text{B1})$$

with the color factor N_c . As usual the former Lorentz structure in above equation is the dominant contribution in the numerical calculations, while the latter Lorentz structure is negligible [68]. In impact coordinate space the B meson wave function can be expressed by [65, 69]

$$\Phi_B(x, b) = \frac{i}{\sqrt{2N_c}} (P_1 + M) \gamma_5 \phi_B(x, b), \quad (\text{B2})$$

where b is the conjugate variable of the transverse momentum of the valence quark of the meson. The distribution amplitude $\phi_B(x, b)$ as being used in Refs. [56, 65] are adopted here

$$\phi_B(x, b) = Nx^2(1-x)^2 \exp\left[-\frac{x^2 M^2}{2\omega_b^2} - \frac{\omega_b^2 b^2}{2}\right], \quad (\text{B3})$$

with the shape parameter ω_b and the normalization constant N being related to the decay constant f_B by normalization:

$$\int_0^1 \phi_B(x, b=0) dx = \frac{f_B}{2\sqrt{2N_c}}. \quad (\text{B4})$$

The shape parameter $\omega_b = 0.40 \pm 0.04$ GeV for the $B_{u,d}$ mesons and $\omega_b = 0.50 \pm 0.05$ GeV for the B_s meson.

For the $\psi(2S)$ meson, the longitudinally and transversely polarized LCDAs up to twist-3 are defined by [49, 50]

$$\begin{aligned} \langle \psi(2S)(P_2, \epsilon_2^L) | \bar{c}(z)_\alpha c(0)_\beta | 0 \rangle &= \frac{1}{\sqrt{2N_c}} \int_0^1 dx e^{ixP_2 \cdot z} [m_{\psi(2S)} \not{\epsilon}_2^L \not{\alpha}_\beta \psi^L(x, b) + (\not{\epsilon}_2^L P_2)_{\alpha\beta} \psi^t(x, b)], \\ \langle \psi(2S)(P_2, \epsilon_2^T) | \bar{c}(z)_\alpha c(0)_\beta | 0 \rangle &= \frac{1}{\sqrt{2N_c}} \int_0^1 dx e^{ixP_2 \cdot z} [m_{\psi(2S)} \not{\epsilon}_2^T \not{\alpha}_\beta \psi^V(x, b) + (\not{\epsilon}_2^T P_2)_{\alpha\beta} \psi^T(x, b)]. \end{aligned} \quad (\text{B5})$$

The asymptotic models for the twist-2 distribution amplitudes $\psi^{L,T}$ and the twist-3 distribution amplitudes $\psi^{V,t}$ are extracted from the correspond Schrödinger states for the harmonic-oscillator potential. Their expressions have been derived as [49].

$$\begin{aligned}\psi^{L,T}(x,b) &= \frac{f_\psi}{2\sqrt{2N_c}} N^{L,T} x \bar{x} \mathcal{T}(x) e^{-x\bar{x} \frac{m_c}{\omega_c} [\omega_c^2 b^2 + (\frac{x-\bar{x}}{2x\bar{x}})^2]}, \\ \psi^t(x,b) &= \frac{f_\psi}{2\sqrt{2N_c}} N^t (x-\bar{x})^2 \mathcal{T}(x) e^{-x\bar{x} \frac{m_c}{\omega_c} [\omega_c^2 b^2 + (\frac{x-\bar{x}}{2x\bar{x}})^2]}, \\ \psi^V(x,b) &= \frac{f_\psi}{2\sqrt{2N_c}} N^V [1 + (x-\bar{x})^2] \mathcal{T}(x) e^{-x\bar{x} \frac{m_c}{\omega_c} [\omega_c^2 b^2 + (\frac{x-\bar{x}}{2x\bar{x}})^2]},\end{aligned}\tag{B6}$$

with

$$\mathcal{T}(x) = 1 - 4b^2 m_c \omega_c x \bar{x} + \frac{m_c (x-\bar{x})^2}{\omega_c x \bar{x}},\tag{B7}$$

where the parameter $\omega_c = 0.20 \pm 0.02$ GeV. $N^i (i = L, T, t, V)$ are the normalization constants and the normalization conditions:

$$\int_0^1 \psi^i(x,0) dx = \frac{f_\psi}{2\sqrt{2N_c}}.\tag{B8}$$

For a light vector meson, the light-cone wave function for longitudinal (L) and transverse (T) polarization are written as [63]

$$\begin{aligned}\Phi_V^L(x_3) &= \frac{1}{\sqrt{2N_c}} [m_V \not{\epsilon}_3^L \phi_V(x_3) + \not{\epsilon}_3^L \not{P}_3 \phi_V^t(x_3) + m_V \phi_V^s(x_3)], \\ \Phi_V^T(x_3) &= \frac{1}{\sqrt{2N_c}} [m_V \not{\epsilon}_3^T \phi_V^v(x_3) + \not{\epsilon}_3^T \not{P}_3 \phi_V^T(x_3) + i m_V \epsilon_{\mu\nu\rho\sigma} \gamma_5 \gamma^\mu \epsilon_3^{T\nu} v^\rho n^\sigma \phi_V^a(x_3)],\end{aligned}\tag{B9}$$

respectively, where $\epsilon_{0123} = 1$ in our convention. Note that v is the moving direction of vector particle. The twist-2 distribution amplitudes are given by

$$\begin{aligned}\phi_V(x) &= \frac{f_V}{\sqrt{2N_c}} 3x(1-x) [1 + a_{1V}^{\parallel} 3t + a_{2V}^{\parallel} 3(5t^2 - 1)/2], \\ \phi_V^T(x) &= \frac{f_V^T}{\sqrt{2N_c}} 3x(1-x) [1 + a_{1V}^{\perp} 3t + a_{2V}^{\perp} 3(5t^2 - 1)/2],\end{aligned}\tag{B10}$$

and those of twist-3 ones are

$$\begin{aligned}\phi_V^t(x) &= \frac{3f_V^T}{2\sqrt{2N_c}} t^2, \quad \phi_V^s(x) = -\frac{3f_V^T}{2\sqrt{2N_c}} t, \\ \phi_V^v(x) &= \frac{3f_V}{8\sqrt{2N_c}} (1+t^2), \quad \phi_V^a(x) = -\frac{3f_V}{4\sqrt{2N_c}} t,\end{aligned}\tag{B11}$$

with $t = 2x - 1$. The vector (tensor) decay constants $f_V (f_V^T)$ together with the Gegenbauer moments [70] are shown numerically in Table VI. Note that positive $a_1^{\parallel,\perp}$ refer to a \bar{K}^{*0} containing an s quark, while for a $K^{*+} (K^{*0})$ with an \bar{s} quark, $a_1^{\parallel,\perp}$ changes sign [71].

-
- [1] I.I.Y. Bigi, A.I. Sanda, Nucl. Phys. B **193**, 85 (1981).
 - [2] T. Aaltonen et al. (CDF Collaboration), Phys. Rev. D. **85**, 072002 (2012).
 - [3] V.M. Abazov et al. (D0 Collaboration), Phys. Rev. D **85**, 032006 (2012).
 - [4] R. Aaij et al. (LHCb Collaboration), Phys. Rev. Lett. **108**, 101803 (2012).
 - [5] Ed. A. J. Bevan, B. Golob, Th. Mannel, S. Prell, and B. D. Yabsley, Eur. Phys. J. C **74**, 3026 (2014).
 - [6] Y. Liu et al. (Belle Collaboration), Phys. Rev. D **78**, 011106(R) (2008).

TABLE VI: Input values of the decay constants and the Gegenbauer moments [70] of the light vector mesons.

Vector	f_V (MeV)	f_V^T (MeV)	a_{1V}^{\parallel}	a_{2V}^{\parallel}	a_{1V}^{\perp}	a_{2V}^{\perp}
ρ	216 ± 3	165 ± 9	–	0.15 ± 0.07	–	0.14 ± 0.06
ω	187 ± 5	151 ± 9	–	0.15 ± 0.07	–	0.14 ± 0.06
K^*	220 ± 5	185 ± 10	0.03 ± 0.02	0.11 ± 0.09	0.04 ± 0.03	0.10 ± 0.08
ϕ	215 ± 5	186 ± 9	–	0.18 ± 0.08	–	0.14 ± 0.07

- [7] R. Aaij et al. (LHCb Collaboration), Phys. Rev. D **88**, 072005 (2013).
[8] J. P. Lees et al. (BABAR Collaboration), Phys. Rev. D **91**, 012003 (2015).
[9] M. Gronau and J. L. Rosner, Phys. Lett. B **666**, 185 (2008).
[10] R. Fleischer, Phys. Rev. D **60**, 073008 (1999).
[11] S. Faller, R. Fleischer and T. Mannel, Phys. Rev. D **79**, 014005 (2009).
[12] R. Aaij et al. (LHCb Collaboration), Eur. Phys. J. C **72**, 2100 (2012).
[13] R. Aaij et al. (LHCb Collaboration), Phys. Lett. B **762**, 253 (2016).
[14] F. Abe et al. (CDF Collaboration), Phys. Rev. D **58**, 072001 (1998).
[15] S. J. Richichi, et al. (CLEO Collaboration), Phys. Rev. D **63**, 031103 (2001).
[16] B. Aubert et al. (BABAR Collaboration), Phys. Rev. D **65**, 032001 (2002).
[17] B. Aubert et al. (BABAR Collaboration), Phys. Rev. Lett. **94**, 141801 (2005).
[18] B. Aubert et al. (BABAR Collaboration), Phys. Rev. D **76**, 031102 (2007).
[19] V. Chobanova et al. (Belle Collaboration), Phys. Rev. D **93**, 031101 (2016).
[20] V. Bhardwaj et al. (Belle Collaboration), Phys. Rev. D **78**, 051104(R) (2008).
[21] R. Aaij et al. (LHCb Collaboration), Nucl. Phys. B **871**, 403 (2013).
[22] R. Aaij et al. (LHCb Collaboration), J. High Energy Phys. **01**, 024 (2015).
[23] R. Aaij et al. (LHCb Collaboration), Phys. Rev. D **85**, 091105(R) (2012).
[24] R. Aaij et al. (LHCb Collaboration), Eur. Phys. J. C **72**, 2118 (2012).
[25] V.M. Abazov et al. (D0 Collaboration), Phys. Rev. D **79**, 111102(R) (2009).
[26] A. Abulencia et al. (CDF Collaboration), Phys. Rev. Lett. **96**, 231801 (2006).
[27] M. Wirbel, B. Stech, and M. Bauer, Z. Phys. C **29**, 637 (1985).
[28] H.-Y. Cheng and K.-C. Yang, Phys. Rev. D **59**, 092004 (1999).
[29] Blaženka Melić, Phys. Rev. D **68**, 034004 (2003).
[30] C. H. Chen and H. N. Li, Phys. Rev. D **71**, 114008 (2005).
[31] H.-Y. Cheng, Y.-Y. Keum, and K.-C. Yang, Phys. Rev. D **65**, 094023 (2002).
[32] W.-S. Hou, M. Nagashima, and A. Soddu, Phys. Rev. D **71**, 016007 (2005).
[33] C. Sharma and R. Sinha, Phys. Rev. D **73**, 014016 (2006).
[34] S. Faller, M. Jung, R. Fleischer, and T. Mannel, Phys. Rev. D **79**, 014030 (2009).
[35] P. Colangelo, F. D. Fazio, and W. Wang, Phys. Rev. D **83**, 094027 (2011).
[36] J.-J. Xie, and E. Oset, Phys. Rev. D **90**, 094006 (2014).
[37] Kristof De Bruyn and Robert Fleischer, J. High Energy Phys **03**, 145 (2015).
[38] P. Frings, U. Nierste, and M. Wiebusch, Phys. Rev. Lett. **115**, 061802 (2015).
[39] Martin Jung, Phys. Rev. D **86**, 053008 (2012).
[40] H.-n. Li and S. Mishima, J. High Energy Phys. **03**, 009 (2007).
[41] J.-W. Li, D.-S. Du, Cai-Dian Lü, Eur. Phys. J. C **72**, 2229 (2012).
[42] X. Liu, Z.-J. Xiao, Phys. Rev. D **89**, 097503 (2014).
[43] X. Liu, H.-n. Li, and Z.-J. Xiao, Phys. Rev. D **86**, 011501 (2012).
[44] S. Stone and L. Zhang, Phys. Rev. Lett. **111**, 062001 (2013).
[45] R. Fleischer, R. Kneijens, and G. Ricciardi, Eur. Phys. J. C **71**, 1798 (2011).
[46] S. Dubnička, A. Z. Dubničková, M. A. Ivanov, and A. Liptaj, Phys. Rev. D **87**, 074021 (2013).
[47] H. N. Li, H. L. Yu, Phys. Rev. Lett. **74**, 4388 (1995).
[48] H. N. Li, Phys. Lett. B **348**, 597 (1995).
[49] R. Zhou, W. F. Wang, G. X. Wang, L. H. Song, C. D. Lü, Eur. Phys. J. C **75**, 293 (2015).
[50] R. Zhou, H. Li, G. X. Wang, Y. Xiao, Eur. Phys. J. C **76**, 564 (2016).
[51] R. Zhou, Ya Li, W. F. Wang, Eur. Phys. J. C **77**, 199 (2017).
[52] X. Liu, W. Wang, and Y. Xie, Phys. Rev. D **89**, 094010 (2014).
[53] G. Buchalla, A. J. Buras, and M. E. Lautenbacher, Rev. Mod. Phys. **68**, 1125 (1996).
[54] M. Beneke, G. Buchalla, M. Neubert, C.T. Sachrajda, Phys. Rev. Lett. **83**, 1914 (1999); M. Beneke, G. Buchalla, M. Neubert, C.T. Sachrajda, Nucl. Phys.B **591**, 313 (2000); M. Beneke, M. Neubert, Nucl. Phys. B **675**, 333 (2003).
[55] C. Patrignani et al. (Particle Data Group Collaboration), Chin. Phys. C **40**, 100001 (2016).
[56] A. Ali, G. Kramer, Y. Li, C. D. Lü, Y. L. Shen, W. Wang, Y. M. Wang, Phys. Rev. D **76**, 074018 (2007).
[57] K. Abe, et al. (Belle Collaboration), arXiv:hep-ex/0308039v1.

- [58] K. Chilikin, et al. (Belle Collaboration), Phys. Rev. D **88**, 074026 (2013).
- [59] Y. Amhis et al. (Heavy Flavor Averaging Group), arXiv:1612.07233v1.
- [60] R. Aaij, et al. (LHCb Collaboration), Phys. Lett. B **747**, 484 (2015).
- [61] A. Ali, J. G. Körner, G. Kramer, and J. Willrodt, Z. Phys. C **1**, 269 (1979); J. G. Korner and G. R. Goldstein, Phys. Lett. B **89**, 105 (1979).
- [62] R. Zhou, Z. T. Zou, Phys. Rev. D **90**, 114030 (2014).
- [63] V. M. Braun and I. E. Filyanov, Z. Phys. C **48**, 239 (1990); P. Ball, V. M. Braun, Y. Koike, and K. Tanaka, Nucl. Phys. B **529**, 323 (1998); P. Ball, J. High Energy Phys. **01** 010 (1999).
- [64] H. N. Li and B. Melic, Eur. Phys. J. C **11**, 695 (1999).
- [65] T. Kurimoto, H. N. Li, and A. I. Sanda, Phys. Rev. D **65**, 014007 (2001).
- [66] H. N. Li and S. Mishima, Phys. Rev. D **80**, 074024 (2009).
- [67] W.F. Wang, H. N. Li, W. Wang, C. D. Lü, Phys. Rev. D **91**, 094024 (2015).
- [68] C. D. Lü and M. Z. Yang, Eur. Phys. J. C **28**, 515 (2003).
- [69] Y. Y. Keum, H. N. Li, A. I. Sanda, Phys. Rev. D **63**, 054008 (2001).
- [70] P. Ball and G. W. Jones, J. High Energy Phys. **03**, 069(2007).
- [71] P. Ball, and R. Zwicky, Phys. Rev. D **71**, 014029 (2005).